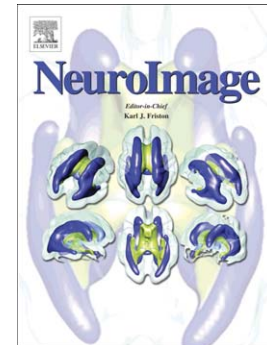# Accepted Manuscript

Beta band modulations underlie action representations for movement planning

Luca Turella, Raffaele Tucciarelli, Nikolaas N. Oosterhof, Nathan Weisz, Raffaella Rumiati, Angelika Lingnau

Please cite this article as: Turella, Luca, Tucciarelli, Raffaele, Oosterhof, Nikolaas N., Weisz, Nathan, Rumiati, Raffaella, Lingnau, Angelika, Beta band modulations underlie action representations for movement planning, *NeuroImage* (2016), doi: 10.1016/j.neuroimage.2016.05.027

Beta Band Modulations underlie Action Representations for Movement Planning

Luca Turella[a], Raffaele Tucciarelli[a], Nikolaas N. Oosterhof[a], Nathan Weisz[a,b], Raffaella Rumiati[c], Angelika Lingnau[a,d,e]*

a. Center for Mind/Brain Sciences (CIMeC), University of Trento, 38123, Italy
b. Centre for Cognitive Neuroscience & Division of Physiological Psychology, University of Salzburg, Austria
c. Scuola Internazionale Superiore di Studi Avanzati (SISSA), 34151, Italy
d. Department of Psychology and Cognitive Science, University of Trento, 38123, Italy
e. Department of Psychology, Royal Holloway University of London, TW20 0EX, UK

* Correspondence:

Dr. Luca Turella

University of Trento - Center for Mind/Brain Sciences (CIMeC)

Via delle Regole, 101

38123, Trento (Italy)

Phone: +39(0)461283098

Email : luca.turella@gmail.com - luca.turella@unitn.it*

Abstract

To be able to interact with our environment, we need to transform incoming sensory information into goal-directed motor outputs. Whereas our ability to plan an appropriate movement based on sensory information appears effortless and simple, the underlying brain dynamics are still largely unknown.

Here we used magnetoencephalography (MEG) to investigate this issue by recording brain activity during the planning of non-visually guided reaching and grasping actions, performed with either the left or right hand. Adopting a combination of univariate and multivariate analyses, we revealed specific patterns of beta power modulations underlying varying levels of neural representations during movement planning. (1) Effector-specific modulations were evident as a decrease in power in the beta band. Within both hemispheres, this decrease was stronger while planning a movement with the contralateral hand. (2) The comparison of planned grasping and reaching led to a relative increase in power in the beta band. These power changes were localized within temporal, premotor and posterior parietal cortices. Action-related modulations overlapped with effector-related beta power changes within widespread frontal and parietal regions, suggesting the possible integration of these two types of neural representations. (3) Multivariate analyses of action-specific power changes revealed that part of this broadband beta modulation also contributed to the encoding of an effector-independent neural representation of a planned action within fronto-parietal and temporal regions.

Our results suggest that beta band power modulations play a central role in movement planning, within both the dorsal and ventral stream, by coding and integrating different levels of neural representations, ranging from the simple representation of the to-be-moved effector up to an abstract, effector-independent representation of the upcoming action.

Key words: Action, MVPA, Grasping, MEG, Motor System, Beta Band.

1. Introduction

In daily life, we continuously interact with objects in our environment. These interactions involve the planning and execution of specific object-directed movements, requiring the representation and integration of different motor parameters, such as the type of action and effector. To date, the brain dynamics underlying these different neural representations are largely unknown.

Neuroimaging studies have identified a fronto-parietal network involved in processing these neural representations, comprising parietal, premotor, and motor cortices (Culham and Valyear, 2006; Culham et al., 2006; Filimon, 2010; Gallivan and Culham, 2015; Grafton, 2010; Turella and Lingnau, 2014; Vesia and Crawford, 2012).

Recent investigations exploited the high sensitivity of multivariate pattern (MVP) analysis to obtain a more fine-grained description of the properties of these neural representations (Gallivan et al., 2013b, 2011b). These studies showed that almost all frontal and parietal regions within this network were sensitive to the subsequently adopted effector (e.g. left vs right hand, *effector coding;* Gallivan et al., 2013b) during movement planning. Moreover, a number of regions within the prehension network, in particular posterior parietal cortex (PPC) and premotor areas, distinguished between different upcoming actions *(action coding)* (Gallivan et al., 2011, 2013b). PPC and premotor regions probably distinguished between these two actions based on the coding of additional sensorimotor transformations required for grasping an object. Several of these regions, particularly within dorsal premotor and PPC, also represented actions at a more abstract level, generalizing across the hand used to perform the movement (*effector independent action coding*, see Gallivan et al., 2013a, 2013b). These results suggest that planned movements are represented at varying levels ranging from the simple representation of the hand to be moved, up to an abstract, effector-independent, representation of the upcoming action.

Despite these advances in the description of the neural basis underlying movement planning, the brain dynamics supporting the coding and integration of these neural representations are not well understood.

Previous human MEG studies associated the beta band with sensorimotor processing during movement planning and execution (Cheyne, 2013). Recent studies extended these findings to more abstract representations, showing modulations of the beta band even if the to be performed action is not known in advance (Tan et al., 2013), and during motor imagery, when no overt movement is performed (Brinkman et al., 2014). Likewise, previous fMRI studies in humans (Gallivan et al., 2013b) and single-cell recording studies in monkeys (Rizzolatti et al., 1988) indicated abstract action representations that generalize across the adopted effector, but so far this issue has not been investigated using MEG.

Prompted by these observations, we predicted that power modulations within the beta band might not only convey concrete information about upcoming movements such as the selected action and the adopted effector, but also more abstract action information that generalizes across the effector. To test this prediction, we used a combination of univariate and multivariate analyses of MEG data.

Using a univariate approach, we aimed at describing beta power modulations associated with the coding of two concrete features during movement planning, the adopted effector and the type of action. To examine whether the two features are hosted in similar brain regions, suggesting their possible integration, we used source analysis.

One limitation of the standard univariate approach is that it cannot directly test the encoding of more abstract information regarding upcoming actions. We therefore used MVP analysis of MEG data, using methods originally developed for fMRI data (for a similar approach, see Tucciarelli et al., 2015). In particular, we used cross-decoding, which consists in training a classifier on a specific subset of data (e.g. movements performed with the left hand) and testing it on another set of data lacking such property (e.g. movements performed with the right hand). The idea behind this approach is that if the model we trained on one hand is able to distinguish between actions performed with the other hand, then the information conveyed by such a model is not bound to the effector performing the action, but resembles a more abstract action coding. Using cross-decoding,

MVP analysis thus allows testing for the generalization of decoding between different actions across different effectors (as shown in fMRI by Gallivan et al., 2013b).

2. Materials and Methods

2.1 Participants

Twenty right-handed participants (13 female) took part in the experiment. All participants gave written informed consent and were paid for their participation in the study. The experimental protocol was approved by the ethics committee for human research of the University of Trento.

2.2 Experimental setup and paradigm

Participants planned and executed non-visually guided grasping or reaching of an object, either with their left or right hand (Figure 1A). The experimental conditions were embedded in a 2x2 factorial design (Figure 1B) with the factors *type of action* (grasping/reaching) and *effector* (left/right hand). Participants were requested either to perform a precision grip using the thumb and the index finger towards an object (grasping) or to touch the same object with the knuckles (reaching). The object was a half-sphere (radius 2.5 cm) positioned centrally on a plastic tray at the same distance (15 cm) from their hands (see Figure 1B). The onset of participant's hand movements was determined via a fiber-optic system which recorded at which time the hand left the starting position. Both object and hands were hidden from the participant's sight by a plastic barrier positioned above the participant's arms (Figure 1A).
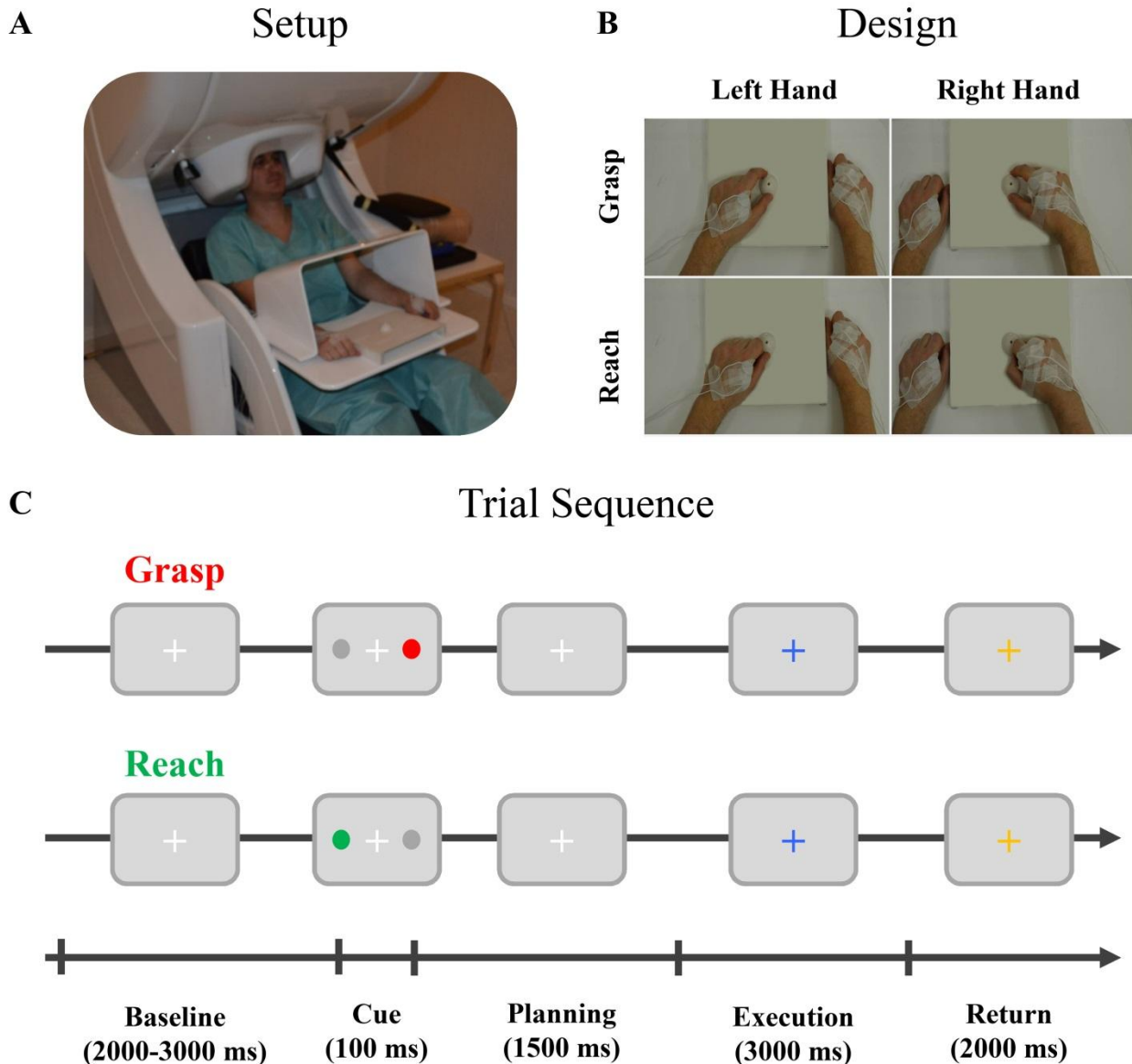
A Setup

B Design

Left Hand   Right Hand

Grasp

Reach

C Trial Sequence

Grasp

| + | • + ● | + | + | + |

Reach

| + | ● + • | + | + | + |

| Baseline (2000-3000 ms) | Cue (100 ms) | Planning (1500 ms) | Execution (3000 ms) | Return (2000 ms) |

Figure 1. A. Setup. Participants performed a delayed movement task in the MEG system following visual instructions projected on a screen. The task consisted in planning and executing non-visually-guided actions on an object positioned centrally on a plastic tray at the same distance from the two hands. The sight of the arms and of the object was hidden to the participant by a white plastic barrier. **B. Design.** The 2x2 factorial design comprised the planning and execution of four non-visually-guided object-directed actions (grasping vs reaching with the left or right hand). **C. Trial Sequence.** Each trial started with a baseline phase, where the participant had to fixate a grey cross. Then, a cue instructed the participant which action to perform (red: grasping, green: reaching) and which effector to move in the subsequent execution phase (indicated by the position of the colored disc). The execution phase started when the fixation cross turned blue. Finally, in the return phase (yellow cross) the participant had to return their hand to the starting position and blink.

2.3 Experimental trial

Participants were requested to follow visual instructions presented on a screen using ASF (Schwarzbach, 2011) based on the MatLab Psychtoolbox-3 for Windows (Brainard, 1997; Pelli, 1997). Stimuli were projected on a screen (1280 x 1024 resolution, 60 Hz refresh rate) that was placed about 130 cm in front of the participants. The screen was visible as a rectangular aperture of about 13.16° x 21.7°. Before starting the experiment, participants practised an entire run both outside and inside the MEG system to familiarize with the task. The experiment consisted of 10 runs, each comprising 48 pseudo-randomly presented experimental trials (12 for each condition, for a total of 120 repetitions per condition per participant). The timing of an experimental trial (Figure 1C) was adapted from a previous study on movement planning (Van Der Werf et al., 2010).

Each trial (for an example, see Figure 1C) started with a baseline phase where the participant had to fixate a grey cross (randomized duration: 2000/ 2500/ 3000 ms). Next, a cue (duration: 100 ms) was presented which consisted of two circles positioned to the left and right of the cross, one colored and one grey. This cue instructed the participant which movement to perform subsequently. The color of the cue indicated the type of action (grasping, reaching) and the position of the cue indicated the effector (cue on the left: left hand, cue on the right: right hand). The assignment of colors to the type of action was counterbalanced across participants. After the disappearance of the cue, the participant kept their hands still while fixating the cross presented in the baseline condition (planning phase, duration 1500 ms). Once the fixation cross turned blue, the execution phase started and the participant had to perform the planned action and to maintain their hand at the final position (execution phase, duration: 3000 ms). The return phase (duration: 2000 ms) started when the cross turned yellow. During this phase, participants had to move the hand back to the initial position and were requested to blink. Then, the subsequent trial started with the grey fixation cross (baseline condition).

2.4 Data acquisition

MEG data were recorded using a 306-channels whole head MEG system (Neuromag Elekta, Finland) at a sampling rate of 1000 Hz. Before entering the MEG room, the individual head shape of each participant was collected using a Polhemus system (Polhemus, Colchester, VT).

Simultaneously to MEG data, eye movement and electromyographic (EMG) data were acquired. Eye movements were recorded using an MEG compatible eye-tracker (Sensomotoric Instruments, Germany; 60 Hz sampling rate) positioned within the MEG room to measure blinks and saccades. To detect possible movements during the planning phase, we recorded EMG from two muscles of each limb (first dorsal interosseus and extensor digitorum communis). In addition, for online and offline control of behaviour, we recorded participants' behaviour using an MEG compatible video camera which was positioned above the participant.

2.5 MEG data preprocessing

MEG data analysis was performed using the FieldTrip toolbox (Oostenveld et al., 2011). Continuous data were high-pass filtered at 1 Hz, low-pass filtered at 120 Hz, notch filtered for line noise (50 and 100 Hz) and downsampled (400 samples per second). Then, epochs of interest were extracted considering the entire experimental trial duration, from the baseline phase (2000 ms before cue onset) until the end of the execution phase (6000 ms from cue onset). Given the aim of the study, we focused on the analysis of the planning phase (between 0 and 1600 ms) for the combined gradiometers only.

Epochs showing any abnormality in the signal within the baseline or planning phase (e.g. jump artefacts, saturated or dead sensors, eye movements) were excluded from further analysis. In addition, we excluded epochs based on behavioural errors performed in the subsequent execution phase, assuming participants did not correctly plan the instructed movement in such trials (e.g. the

participants grasped the object instead of reaching it), or if participants moved the hand during the planning phase. On average, we excluded 15.86 % of all trials from further analysis. Sensors showing noisy activity throughout the entire experimental session were rejected and reconstructed by interpolating neighboring sensors. This procedure ensured having the same number of sensors for all participants.

2.6 Behavioural data analysis

Analysis of behavioural performance was conducted on the non-discarded epochs for all the participants. We extracted reaction times (RTs) of the movements performed during the execution phase, even if this phase was not the focus of the present study (see Table 1). RTs were defined as the time interval between the appearance of the go cue (blue cross) and the time point at which the hand was released from the starting position (recorded using the fiber-optic system). A 2x2 repeated measure ANOVA was performed to assess any significant effect at group level. RTs were neither modulated by the type of action [$F_{(1,19)}$= 2.806, p=0.11] nor by the effector [$F_{(1,19)}$= 0.522, p=0.425] or their interaction [$F_{(1,19)}$= 0.379, p=0.546].

		Effector	
		Left	Right
Type of Action	**Grasp**	540.45±22.99	535.01±22.47
	Reach	554.10±22.18	542.60±21.60

Table 1. Mean and standard error of the mean values for reaction times are reported.

2.7 Univariate analysis of time frequency data

We computed time–frequency representations (TFRs) using a Fourier approach. The analysis was carried out within a specific frequency range (5-30 Hz) by applying a sliding window of 500

ms and a Hanning taper (with time points spaced every 50 ms). TFRs of changes in power for each condition were computed with respect to average power within a period of the baseline phase (from -1600 to -100 ms) considering all the non-rejected epochs.

All statistical analyses on power changes at the sensor level were performed using a non-parametric method based on a Monte Carlo simulation approach with 1000 randomizations (Maris and Oostenveld, 2007). P values were set at p<0.05 for single comparisons. To control for multiple comparisons, we used cluster level correction with p<0.05 (based on the sum of the t-values, see Maris and Oostenveld, 2007). For statistical comparisons, we considered at least two neighboring sensors when clustering at the sensor level.

Previous human EEG/MEG studies demonstrated time-frequency (TF) power modulations within the beta band during hand movement planning and execution (Verhagen et al., 2012; Virji-Babul et al., 2010; Wheaton et al., 2009, 2005; Zaepffel et al., 2013). Based on the results of the study by Zaepfell and colleagues (2013), adopting an experimental paradigm similar to ours, we focused on a specific range within the beta band (15-25 Hz).We first identified the sensors where power changes over time within the beta band were significantly different for both main effects (i.e. type of action and effector) by defining clusters of significant power modulations within the planning phase (in steps of 50 ms). Next, we extracted any sensor that was significant within the identified time period in order to define the sensor topography for the two main effects. In addition, to examine power modulations within a broader range of frequencies (between 5 and 30 Hz) for the entire planning phase, we plotted power modulations within the sensors of the identified topographies.

2.8 Source analysis reconstruction

We built a subject-specific anatomical image by warping an MNI template brain to fit the individual head shape collected before the beginning of the MEG session using the Polhemus system (Polhemus, Colchester, VT). Then, for every participant we warped this anatomical image to fit the MNI template brain and a 1-cm three-dimensional grid built within the same MNI space. This grid was then warped back to fit each participant's original anatomical image, so that in each participant the same grid point resembles the same MNI coordinates.

For each participant, we used a volume conductor model using the single-shell method (Nolte, 2003). The neural sources generating the two main effects were localized by applying a beam-forming technique (Dynamic Imaging of Coherent Sources, DICS; Gross et al., 2001). Source reconstruction was performed considering the value of the peak power change and the significant time period. We applied DICS separately for each condition using a common spatial filter computed from the combination of all the conditions. This was done to ensure that any difference between the conditions could not be attributed to differences between the filters. Source images were interpolated from the original resolution onto an inflated surface of an MNI template brain available within the Caret software package (Van Essen et al., 2001, http://brainvis.wustl.edu/wiki/index.php/Caret:About). For visualization purposes, we thresholded the resulting maps to show only 10% of the grid points with maximum power change (for a similar approach see Tucciarelli et al., 2015).

2.9 Multivariate pattern (MVP) analysis of sensor and source data

We used cross-decoding multivariate analysis (Ariani et al., 2015; Gallivan et al., 2013a, 2013b; Oosterhof et al., 2012a, 2012b, 2010; Tucciarelli et al., 2015; Wurm and Lingnau, 2015; Wurm et al., 2015) to examine if action-specific power modulations also conveyed an effector-

independent neural representation of action. Cross-decoding consisted in training a model on data from one effector and testing it on another set of data from the other effector, i.e. effector-independent action encoding (Gallivan et al., 2013a, 2013b).

For MVP analysis, we used a Support Vector Machine (SVM) classifier (LIBSVM, http://www.csie.ntu.edu.tw/~cjlin/libsvm/, Chang and Lin, 2011) available in the CoSMoMVPA Toolbox (Oosterhof et al., in prep., http://www.cosmomvpa.org/), choosing a linear kernel and a constant cost parameter (C=1). For each participant, we carried out cross-decoding MVP analysis on (z-scored) single trial power data both in sensor and source space (for a schematic overview see Figure 2 and 3).

The classifier used different features for sensor and source space (for a similar approach, see Tucciarelli et al., 2015). At sensor level, we based our decoding analysis on univariate TFRs of power data adapting a searchlight method used in fMRI data analysis (Kriegeskorte and Bandettini, 2007; Oosterhof et al., 2011). The approach consisted in performing a sensor-based multivariate decoding analysis in a feature space defined in time × frequency band space. The searchlight used power values calculated in the univariate analysis as features for the classifier, selecting only the values coming from the sensors found significant at group level in the pairwise comparison used to train the classifier (Figure 2, step 1).

For each feature (in time × frequency band space), we defined a neighborhood by taking the power values across neighboring time points (± 2 time bins of 50 ms) and frequency bins (± 2 frequency bins of 1 Hz) from all the selected sensors (Figure 2, step 2). Classification accuracies for each neighborhood were then assigned to the originally selected feature. We used a cross-validation approach to estimate decoding accuracy. For the first cross-validation fold (Figure 3, step 3), we trained a classifier on the pairwise comparison, grasping vs reaching with the right hand, and testing it on grasping vs reaching with the left hand. The result of the cross-validation fold for this multivariate searchlight analysis is a classification accuracy map in time × frequency band space

(Figure 2, step 4). For the second cross-validation fold (Figure 2, step 5), the process was repeated after swapping the data used for training and testing across the two hands (training on left hand, testing on right hand). Within each of the two cross-validation folds, we used all the trials of the specific pairwise comparisons for training the classifier and all the trials of the other pairwise comparisons for testing the classifier. If the number of trials within the training set was not the same for each condition, as a result of our trial rejection procedure, we randomly selected the same number of trials from both conditions. For each participant, we averaged the TF decoding maps obtained from the two cross-validation fold (Figure 2, step 6).

This average map can be tested for information discriminating between conditions at the group level, as in normal univariate TF analysis, by comparing the resulting accuracy maps against chance level (50 %) using a non-parametric approach implemented in the CoSMoMVPA Toolbox (Oosterhof et al., 2016) adopting 10000 permutations (see http://cosmomvpa.org/matlab/cosmo_montecarlo_cluster_stat.html). P values were set at p<0.05 for cluster level correction to control for multiple comparisons adopting Threshold-Free Cluster Enhancement (Smith and Nichols, 2009) with the suggested default values (H=2, E=0.5, dh=0.1) which have been recently validated for MEG/EEG data (Pernet et al., 2015).

SENSOR-BASED MULTIVARIATE ANALYSIS WORKFLOW

SINGLE SUBJECT LEVEL

---

1. GROUP LEVEL SENSOR SELECTION
(based on pairwise comparison used for training the classifier)

↓

2. DEFINE SEARCHLIGHT IN TIME-FREQUENCY BAND SPACE
Features: single trial power data from selected sensors
Neighborhood: selected feature ±100 ms and ±2 Hz

↓

3. ESTIMATE DECODING ACCURACY

TRAIN CLASSIFIER ON PAIRWISE COMPARISON 1
(e.g. grasping vs reaching with the right hand)

TEST CLASSIFIER ON PAIRWISE COMPARISON 2
(e.g. grasping vs reaching with the left hand)

↓

4. TF DECODING MAP FOR CROSS-VALIDATION FOLD

↓

6. AVERAGE TF DECODING MAPS OBTAINED FROM THE TWO CROSS-VALIDATION FOLDS

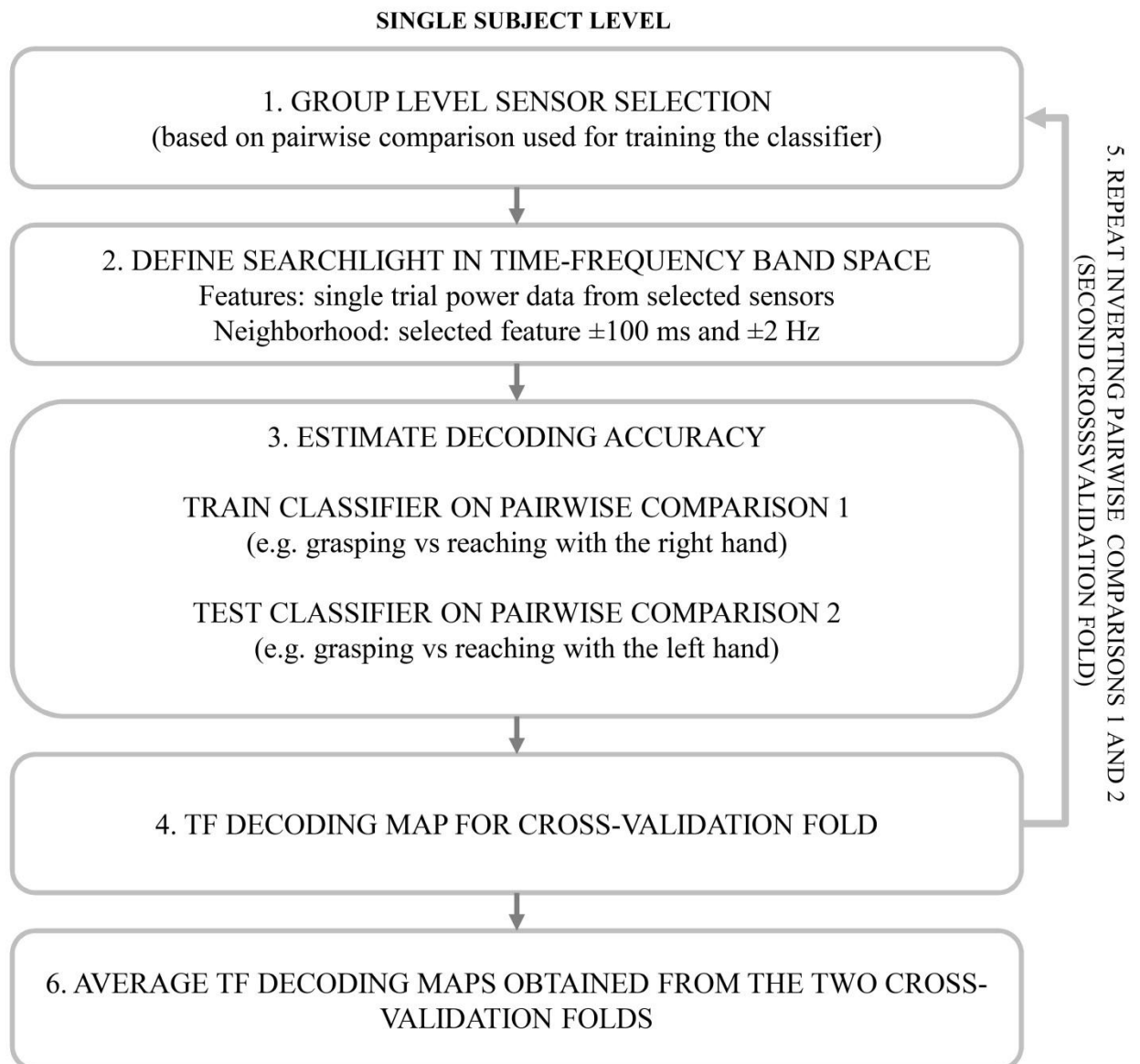*5. REPEAT INVERTING PAIRWISE COMPARISONS 1 AND 2 (SECOND CROSSVALIDATION FOLD)*

Figure 2. Sensor-based Multivariate Analysis Pipeline. Step 1. Define univariate sensors significant for pairwise comparison used to train the classifier at group level (e.g. grasping vs reaching with right hand in the time window between 750-1050 for beta band 15-25 Hz). Step 2. Define searchlight in time frequency band space using z-scored power values for all the selected sensors defined in step 1. For each feature, define a neighborhood (± 100 ms and ± 2 Hz) taking power values from all the selected sensors. Step 3. Estimate decoding accuracy for each neighborhood. Train SVM classifier on the selected pairwise comparison 1 (e.g. grasping vs reaching with right hand). Test the SVM-classifier on the pairwise comparison 2 (e.g. grasping vs reaching with left hand). Classification accuracies for each neighborhood were then assigned to the originally selected feature. Step 4. Obtain a TF decoding map for the tested cross-validation fold. Step 5. Adopt the same procedure (steps 1-4) inverting the pairwise comparisons used for defining

and training with respect to testing (define and train using grasping vs reaching with left hand, test grasping vs reaching with right hand). Step 6. Average the two decoding maps for each subject.

To determine the sources underlying the cross-decoding effect found at sensor level, we carried out an additional MVP analysis on power data at source level (i.e. multivariate source analysis, see Figure 3 for an overview of the analysis workflow). For each participant, the procedure involved the extraction of source power data on a single trial basis using a DICS beamforming technique based on the peak of decoding found using sensor-based multivariate analysis. Briefly, the trials for all conditions were used to create a common filter which was subsequently used to extract single trial source power data. MVP analysis was performed using a searchlight approach, i.e. performing multiple separate multivariate decoding analyses along all the positions within the source space (i.e. 1 cm-spaced grid in MNI space) and assigning the resulting decoding value to each selected grid point. The searchlight was defined using the power values of the selected grid point and of the surrounding neighboring ones within a radius of 2 cm (Figure 3, step 1). The searchlight was then applied to single trial data separately for each participant, resulting in a source map in MNI space with decoding accuracy as dependent measure. Also here, a cross-validation approach comprising two folds was adopted to estimate decoding accuracy (Figure 3, step 2-3-4), as in the case of sensor-based multivariate analysis. The adopted pairwise comparisons were the same as in the sensor analysis: grasping vs reaching with the right hand and grasping vs reaching with the left hand. For each subject, the decoding maps of the two cross-validation folds were averaged (Figure 3, step 5).

For visualization purposes, similarly to our approach for univariate source analysis, we plotted the source maps for average decoding accuracy on an inflated brain surface thresholded to show only grid points with 10% maximum decoding accuracy (see for a similar approach, Tucciarelli et al., 2015).

MULTIVARIATE SOURCE ANALYSIS WORKFLOW

SINGLE SUBJECT LEVEL

1. DEFINE SEARCHLIGHT IN SOURCE SPACE
Features: single trial source power data
Neighborhood: selected grid point and surrounding sphere (radius=2cm)

2. ESTIMATE DECODING ACCURACY

TRAIN CLASSIFIER ON PAIRWISE COMPARISON 1
(e.g. grasping vs reaching with the right hand)

TEST CLASSIFIER ON PAIRWISE COMPARISON 2
(e.g. grasping vs reaching with the right left)

3. SOURCE DECODING MAP FOR CROSS-VALIDATION FOLD

5. AVERAGE SOURCE MAPS OBTAINED FROM THE TWO CROSS-VALIDATION FOLDS

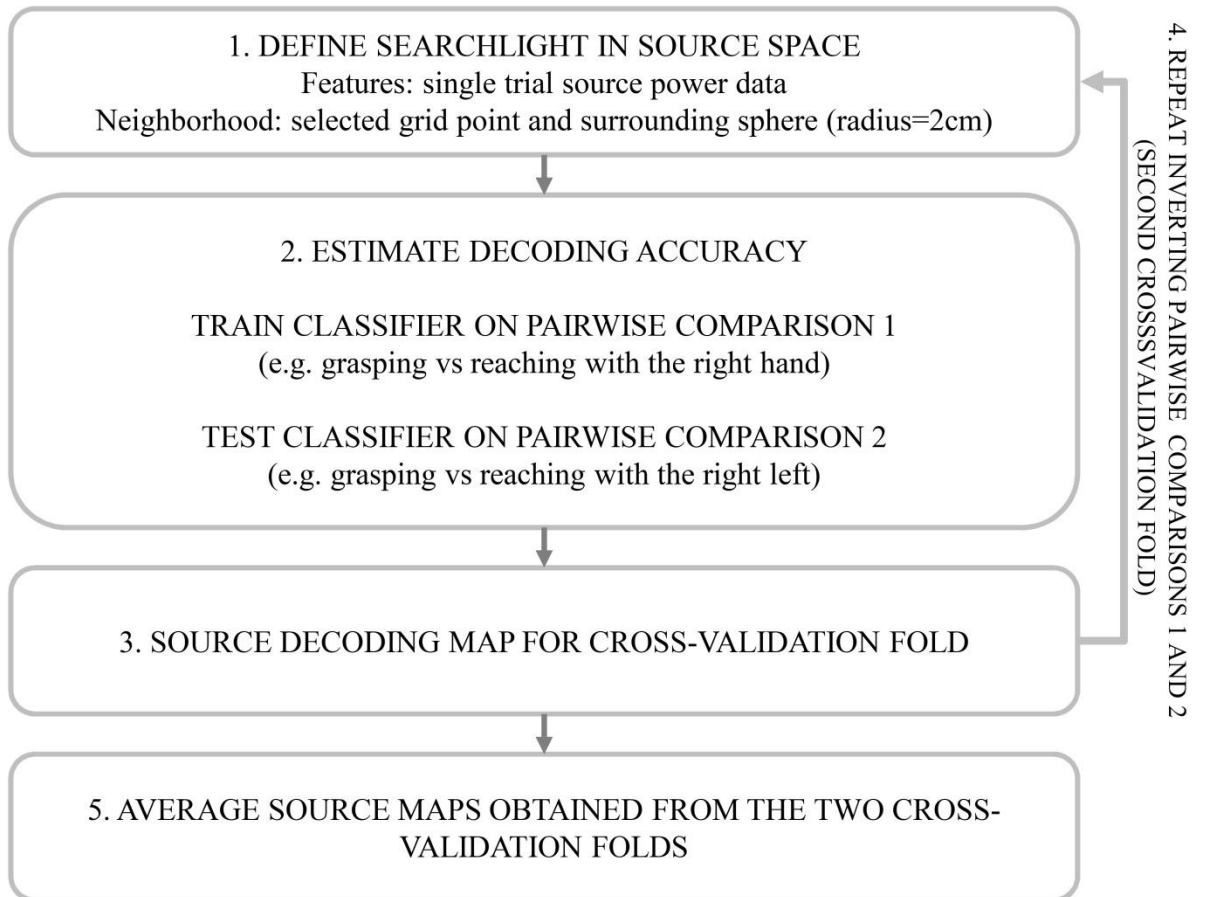4. REPEAT INVERTING PAIRWISE COMPARISONS 1 AND 2 (SECOND CROSSSVALIDATION FOLD)

Figure 3. Multivariate Source Analysis Pipeline. Step 1. Define searchlight in source space using z-scored single trial source power trials. For each feature, define a neighborhood comprising selected grid point and surrounding grid points within a sphere of 2 cm. Step 2. Estimate decoding accuracy for each neighborhood. Train SVM classifier on the selected pairwise comparison 1 (e.g. grasping vs reaching with right hand). Test the SVM-classifier on the pairwise comparison 2 (e.g. grasping vs reaching with left hand). Classification accuracies for each neighborhood were then assigned to the originally selected grid point. Step 3. Obtain a TF decoding map for the tested cross-validation fold. Step 4. Adopt the same procedure (steps 1-3) inverting the pairwise comparisons used for defining and training with respect to testing (define and train using grasping vs reaching with left hand, test grasping vs reaching with right hand). Step 5. Average the two decoding maps for each subject.

To assess generalization of effector encoding across the type of action, i.e. action-independent effector coding, we adopted an approach similar to the effector-independent action decoding (see

above) at both sensor and source levels (see Figure 2 and 3, but adopting different pairwise comparisons). For the first cross-validation fold, we trained a classifier on a pairwise comparison between two conditions for the reaching action, performed with left vs. right hand, and tested on the grasping action. For the second cross-validation fold, the process was repeated after swapping the data used for training and testing across type of action.

3. Results

3.1 Effector coding: univariate analysis of TFRs and source localization

We computed power modulations for *effector coding*, i.e. planning left vs. right hand movements. Significant power modulations within the beta band were evident after 250 ms from cue onset and persisted throughout the entire planning phase (Figure 4A, lateral panels). The average topography of this effect was localized within two clusters, roughly corresponding to the two hemispheres (see Figure 4A, central panel).

We observed a bilateral decrease of power, but this modulation was stronger within each hemisphere for planning movements with the contralateral hand. This behavior is evident within the TFRs extracted from the significant sensors for each hemisphere (Figure 4A, lateral panels). Effector-specific TF modulations were not limited to the beta band, but also extended to the alpha band (Figure 4A, lateral panels) which showed a similar pattern of bilateral decrease with a stronger reduction in power for movements planned with the controlateral effector.

For visualization purposes, we applied source analysis considering the significant time period of the planning phase (250 – 1600 ms) within a broad beta band interval (20 ± 5 Hz). Sources generating this effect were widely distributed within the fronto-parietal prehension network, comprising premotor cortices (PMd, PMv and SMA), primary motor and somatosensory regions, and cortical areas within the PPC (Figure 4B).

EFFECTOR CODING DURING MOVEMENT PLANNING

A Univariate Analysis
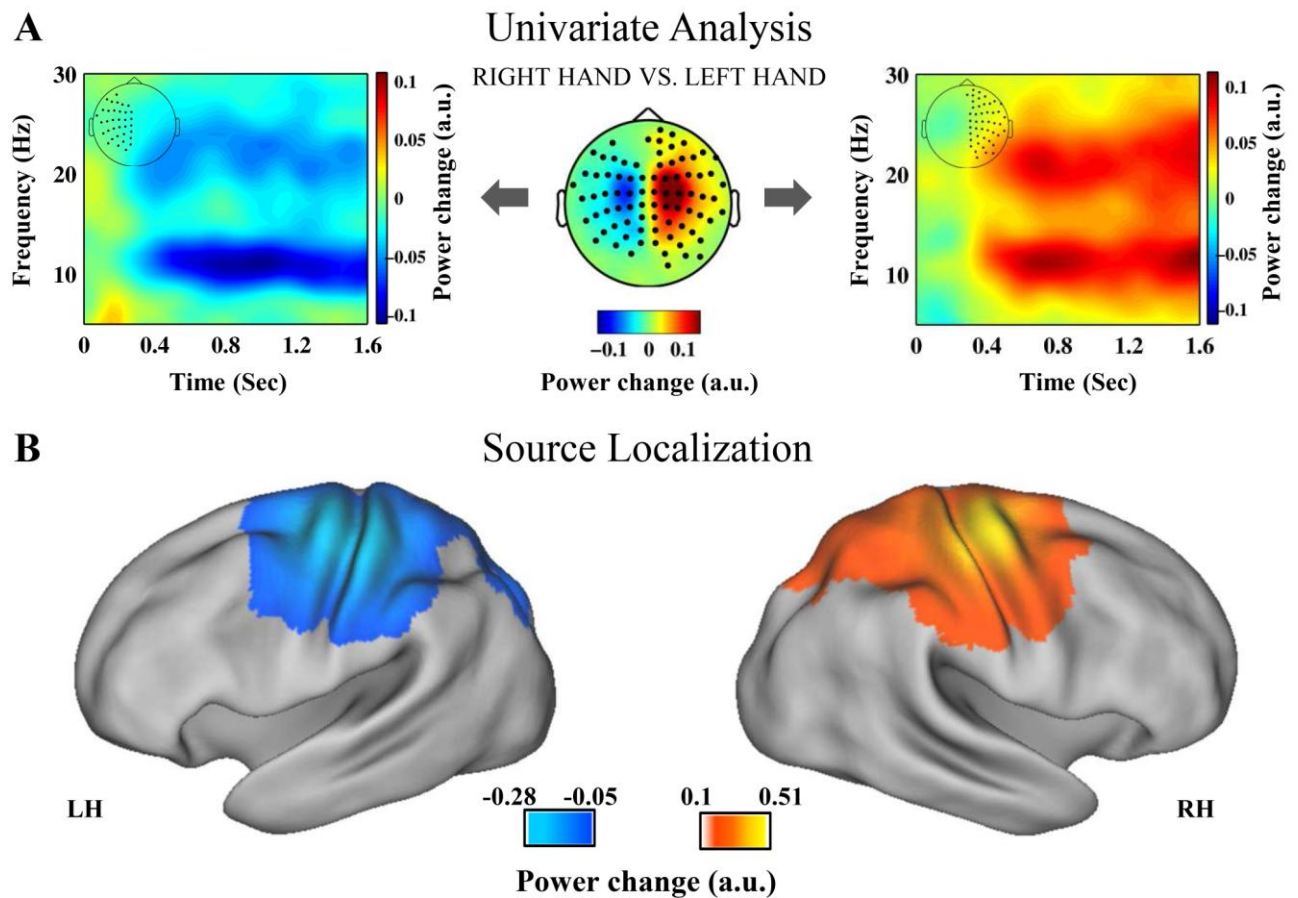

B Source Localization

Figure 4. A. Topography and Clusters' TFRs for effector coding. The central topography represents any sensor significant for effector coding (right vs left hand) within the significant time period (250-1600 ms). The plot represents mean power change of the sensors averaging across the significant time period within the beta band (15-25 Hz). The two upper lateral panels represent mean TFRs of the sensors within the two clusters showing relative power change defined in arbitrary units (a.u.), as right hand-left hand. **B. Source Localization.** Localization of sources for effector coding is projected on the two lateral views of the brain. Relative power modulations were defined as (right hand-left hand)/left hand. Only 10 % of the grid points with maximum and minimum power change (below 5th and above 95th percentile) are depicted. Source maps have been projected on an inflated brain template adopting the Caret software (Van Essen et al., 2001, http://brainvis.wustl.edu/wiki/index.php/Caret:About). LH, left hemisphere; RH; right hemisphere.

3.2 Action coding: univariate analysis of TFRs and source localization

Action-specific power changes were evident within the beta band between 750 and 1050 ms after cue onset. The average topography of *action coding* was localized within two clusters (Figure 5A, central panel) showing a relative increase in beta power for planning grasping actions with respect to reaching. These sensors were a subset of those found modulated by the effector main effect, suggesting that the two effects are overlapping in sensor space. We extracted the TFRs from the two clusters. In both clusters there was a clear broadband beta power increase in the significant time period (750-1050 ms, Figure 5A).

This timing of recruitment seems to be compatible with recent fMRI results showing the possible decoding of grasping vs reaching actions at the end of the planning phase, just before the go cue (Gallivan et al., 2013b, 2013c). This seems to suggest that if participants can predict the timings of the experimental task, as in our study, action representations might be recruited just before the time the participants know they should perform the action. In contrast, effector-related power modulations are present throughout the entire planning phase (see effector coding section).

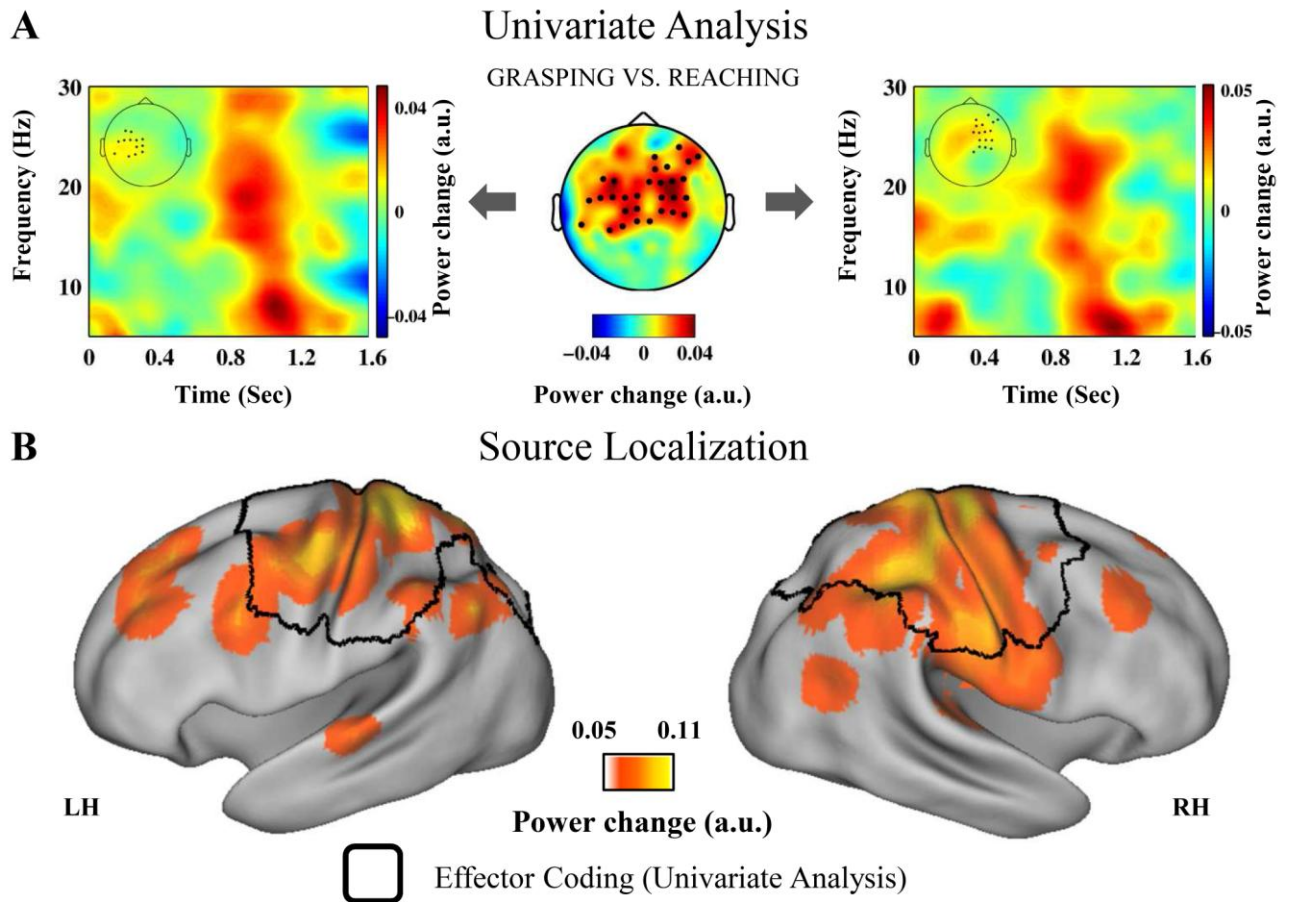## ACTION CODING DURING MOVEMENT PLANNING

Figure 5. A. Univariate results for action coding (Grasping vs. Reaching). The central topography represents any significant sensor for the action type main effect (grasping vs. reaching) within the significant time period (750-1050 ms). The plot represents mean power change of the sensors averaging across the significant time period within the beta band (15-25 Hz). The two upper lateral panels represent the mean TFRs of the sensors within the two clusters depicted within the insets. Relative power change was expressed in arbitrary units (a.u.) calculated as grasping - reaching. **B. Source estimation.** Visualization of sources for action coding is projected on the two lateral views of the brain. Relative power modulations were defined as: (grasping - reaching)/reaching. Only 10 % of the grid points with maximum power change (above 90th percentile) are depicted. Source maps have been projected on an inflated brain template adopting the Caret software (Van Essen et al., 2001, http://brainvis.wustl.edu/wiki/index.php/Caret:About). To be able to compare the effects of effector and action coding, the borders of the significant sources for effector coding (univariate analysis) depicted in Figure 4C have been projected on the brain surface as a black outline. **LH**, left hemisphere; **RH**; right hemisphere.

For visualization purpose, we performed source analysis selecting the significant time period (750-1050 ms) and frequency range (20 ± 5 Hz). As the comparison grasping vs. reaching was significant only in the positive direction (Figure 5A, central panel), we focused on sources generating this type of power modulation, which were found in the temporal cortex and bilaterally in the ventral (PMv) and dorsal (PMd) premotor cortices, dorsolateral prefrontal cortex, PPC and precuneus (Figure 5B). Furthermore, Figure 5B suggests a spatial overlap between areas coding effector and action type in bilateral motor, somatosensory, premotor (PMv, PMd, SMA) and PPC regions.

3.3 Effector-independent action coding: multivariate analysis of sensor and source data

As described above, previous studies using MVP analysis of fMRI data identified *effector-independent action* representations within a wider set of cerebral regions showing *action coding* (Gallivan et al., 2013b). Based on these findings (Gallivan et al., 2013b), we expected that action-specific beta activity might also convey information underlying an abstract representation of the upcoming action, i.e. irrespective of the hand used to perform the movement.

Following these assumptions, we chose to focus on the significant sensors identified with the univariate contrast for action coding. However, the main effect of action coding might highlight sensors where power modulations for grasping with both hands might be higher than the respective reaching condition. Using significant sensors from both hands could thus lead to circular analysis problems (see Kriegeskorte et al., 2009). To avoid this possibility, we identified significant sensors specific for grasping actions performed with each hand separately (right grasping vs. right reaching, left grasping vs. left reaching) by performing a univariate comparison within the same time window (750-1050 ms) and frequency band (15-25 Hz) identified for the action type main effect (Figure 2, step 1). Next, we performed two sensor-based multivariate analyses, one for each cross-validation

fold, using power values for all the significant sensors as features for the classifier and performing a searchlight in time x frequency space (Figure 2, step 2). We tested each cross-validation fold, using the pairwise comparison adopted to localize the sensors in the univariate analysis for training, and the other pairwise comparison for testing obtaining a decoding TF map (Figure 2, steps 3-4-5). Then, we averaged the decoding TF maps of the two cross-validation folds obtained for each participant (Figure 2, step 6) and tested the obtained accuracy maps against chance decoding at group level. We found significant cross-effector decoding (surviving TFCE multiple comparison correction at cluster level) within the low beta range below 20 Hz (see Figure 6A).

For visualization purpose, we localized sources with above chance decoding adopting an additional multivariate analysis at source level (see Figure 3) extracting single trial data from the peak of decoding found using the sensor-based MVP analysis (18 ± 3 Hz, time window: 700-1100 ms). The result of this analysis demonstrated that cross-effector decoding for grasping actions was localized bilaterally within premotor cortices (PMv, PMd and SMA), intraparietal sulcus and temporal cortex (see Figure 6B). Furthermore, within the left hemisphere there was also the involvement of the inferior frontal gyrus and the dorsolateral prefrontal cortex.

EFFECTOR-INDEPENDENT ACTION CODING

A   Sensor-Based Multivariate Analysis

z = 1.65 (p=0.05 corr.)
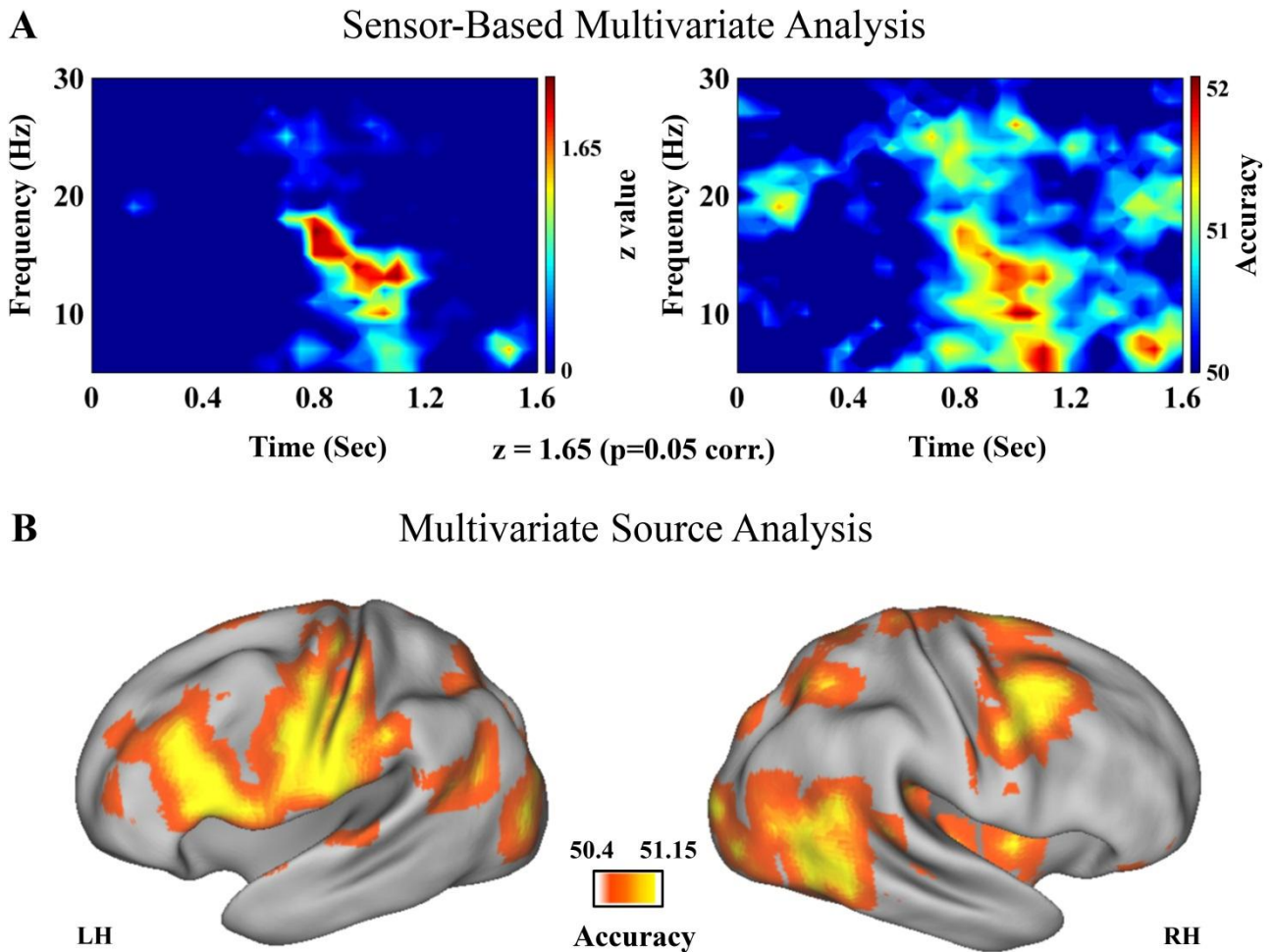
B   Multivariate Source Analysis

Figure 6. A. Sensor-based multivariate analysis for effector-independent action coding. Multivariate searchlight analysis was performed in time x frequency space considering as features power values extracted from all the significant sensors identified at univariate level for each cross-validation fold separately. Decoding results for the average of the two cross-validation folds are presented. The TFR on the left depicts z-values assessing the statistical significance of decoding accuracies (z value of 1.65 corresponds to p=0.05 TFCE corrected). On the right, TFR with raw decoding accuracy values averaged across participants is depicted without any statistical masking. **B. Multivariate source analysis for effector-independent action coding**. On the two lateral views of the brain, the localization of regions showing above chance decoding for action type cross-decoding is depicted. Only 10% of the grid points with maximum decoding value (above 90th percentile) are shown. Source maps have been projected on an inflated brain template adopting the Caret software (Van Essen et al., 2001, http://brainvis.wustl.edu/wiki/index.php/Caret:About). **LH**, left hemisphere; **RH**, right hemisphere.

3.4 Action-independent effector coding: multivariate analysis of sensor and source data

To validate our multivariate approach, we adopted MVP analyses of sensor and source power to investigate action-independent effector coding using the same cross-decoding approach used for effector-independent action coding (Figure 2). At sensor space, we directly investigated the decoding performing the searchlight in time x frequency space separately for the two cross-validation folds within the selected sensors (see Figure 3). The only difference was in the adopted pairwise comparisons: left grasping vs right grasping and left reaching vs. right reaching.

Decoding TF maps were statistically tested at group level by adopting the non-parametric approach implemented in the CoSMoMVPA Toolbox (described above), correcting for multiple comparisons with TFCE (see Figure 7A, left panel). Comparing uni- and multivariate TF analysis (Figure 4A, lateral panels and Figure 7A, right panel) for this effect demonstrated that the two analyses revealed qualitatively similar patterns of results.

For visualization purposes, multivariate source analysis was also performed on the beta band adopting the same parameters as in the univariate analysis (time: 250-1600 ms, frequency: 20 ± 5 Hz). The results show bilateral encoding localized within posterior parietal, somatosensory, premotor and motor cortices (Figure 7B). For ease of comparison, the outlines of the corresponding source analysis for the univariate analysis are superimposed (see Figure 7B).

ACTION-INDEPENDENT EFFECTOR CODING

A Sensor-Based Multivariate Analysis

z = 1.65 (p=0.05 corr.)

B Multivariate Source Analysis

52.71   55.08

Accuracy

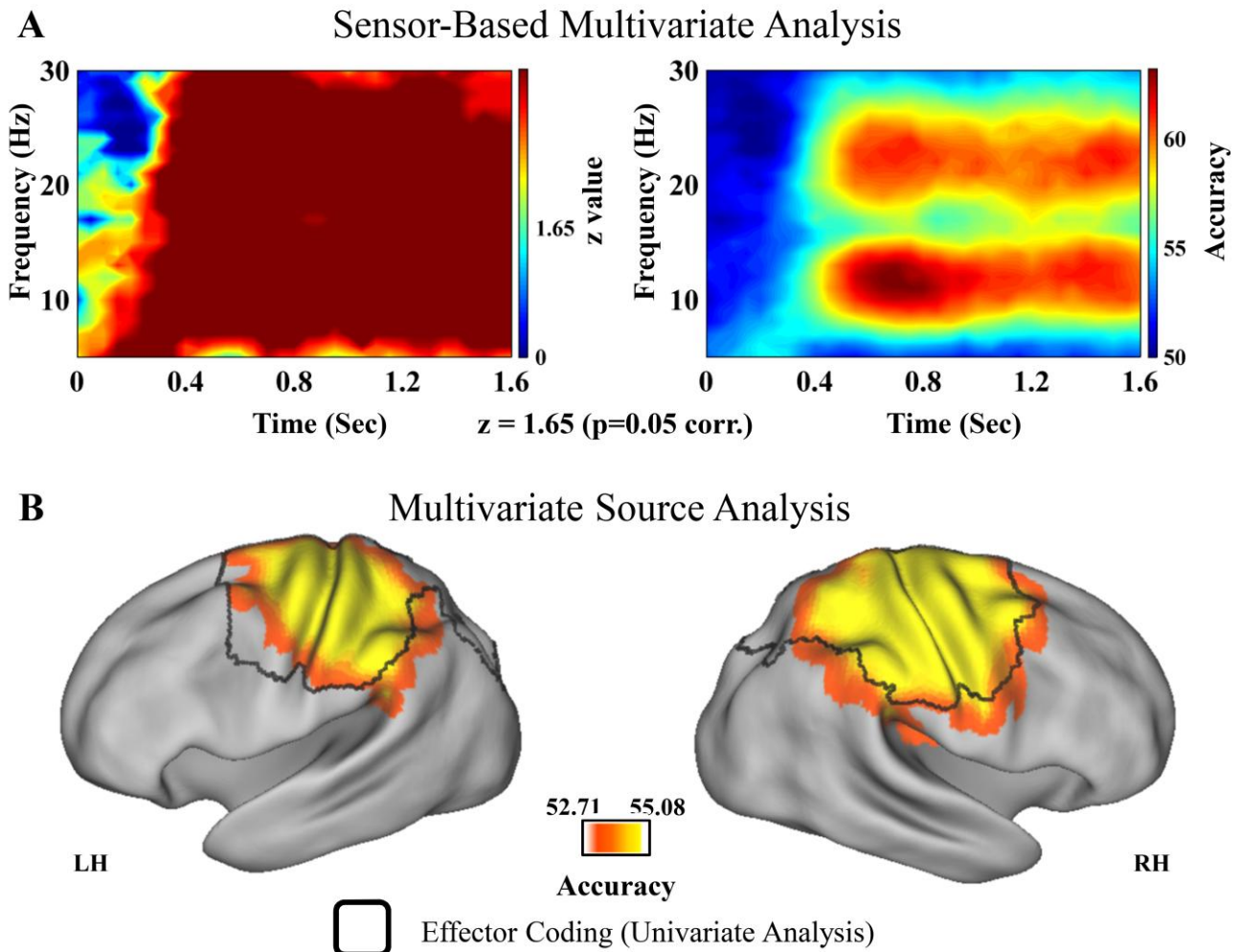☐ Effector Coding (Univariate Analysis)

Figure 7. A. Sensor-based multivariate decoding analysis for action-independent effector coding. Multivariate searchlight analysis was performed in time x frequency space considering as features power values extracted from all the significant sensors identified at univariate level for each cross-validation fold separately. Decoding results for the average of the two cross-validation folds are presented. The TFRs on the left depicts z-values (TFCE corrected) assessing the statistical significance of decoding accuracies (z value of 1.65 corresponds to p=0.05 TFCE corrected). On the right panel, TFR with raw decoding accuracy values averaged across subjects is depicted without any statistical masking. **B. Source decoding analysis.** On the two lateral views of the brain, the localization of regions showing above chance decoding for the average of the two cross-validation folds within the beta band (15-25 Hz) is depicted. Only 10% of the grid points showing maximum above chance decoding (above 90th percentile) are shown. Source maps have been projected on an inflated brain template adopting the Caret software (Van Essen et al., 2001, http://brainvis.wustl.edu/wiki/index.php/Caret:About). The borders of the significant sources for effector coding (univariate analysis) are projected on the inflated brains as a black outline for ease of comparison between the two analyses. **LH**, left hemisphere; **RH**, right hemisphere.

4. Discussion

We found that movement planning was characterized by distinct power modulations within the beta band. Specifically, *effector coding* and *action coding* were represented by a relative decrease and increase, respectively. Whereas *effector coding* was evident throughout most of the planning phase, *action coding* was obtained in a more narrow time window from 750 to 1050 msec after the onset of the cue. These modulations in beta power were evident within overlapping regions in premotor and posterior parietal cortex, suggesting the possible integration of action and effector information within these areas. Moreover, we found that abstract, effector-independent action-related information is encoded within a more narrow frequency band (below 20 Hz) within the broadband beta band modulation described for *action* coding. Sources encoding this abstract information were evident not only within the fronto-parietal prehension network, but also in the ventral stream.

In the next sections, we will discuss the role of beta band modulations in coding these different types of neural representations and their more general role in motor control.

4.1 Role of beta band power modulations in representing effector and action information

Within the general decrease in power obtained during movement planning, the beta band was modulated both by the effector and the type of action. The spatial and temporal overlap between action and effector coding at sensor and source levels suggested that power modulations within the beta band might code two different motor features through a combination of simultaneous relative increase and decrease in power within the same cortical region. These different power changes seem to support the view of beta band power modulations as reflecting the summation of different processes rather than a unitary phenomenon (Kilavik et al., 2013).

At first sight, the demonstration of less beta suppression when comparing grasping with respect to reaching might sound counterintuitive, given the general notion that a stronger decrease in alpha/beta band power implies a stronger recruitment of the motor system (Cheyne, 2013; Neuper et al., 2006).

Similar to our results, a recent MEG investigation on reaching movements (Tzagarakis et al., 2010) described a relative increase in beta power during movement planning. Participants had to plan reaching movements based on a variable number of potential targets. A higher number of potential targets led to a less pronounced beta suppression: maximal decrease was present for one target, with a smaller decrease for two, and an even smaller decrease for three targets. This result supports the idea that a smaller (i.e. relative increase) beta power suppression might be indicative of a planning process requiring higher sensorimotor demands.

Spinks et al. (2008) recorded local field potentials from monkey PMv and motor cortex and showed a similar power increase in the beta band (around 20 Hz) during the planning phase before an upcoming grasp. The effect was partially selective to the grip needed to grasp an object, suggesting a possible role of this power modulation in processing different types of grasp-related information: object shape and spatial position, object affordance, grip type or the transformations needed to convert object shape into a suitable grasping pattern (see also Vargas-Irwin et al., 2015).

Linking these two pieces of evidence, we suggest that the relative increase in beta power might be related to additional sensorimotor transformations required while planning a prehension action, comprising both reaching and grasping, with respect to planning a reaching-only action, such as the appropriate hand shape and wrist orientation.

Most of the regions coding for grasping movements in the current study are in line with previous studies adopting a variety of techniques spanning from human fMRI (e.g. Ariani et al., 2015; Gallivan et al., 2013b, 2011b; Leo et al., 2016), neurostimulation data (e.g. Koch et al., 2010;

Vesia et al., 2013) and monkey single cell recordings (Baumann et al., 2009; Bonini et al., 2012, 2011, 2010; Brochier and Umiltà, 2007; Fattori et al., 2012, 2010, 2009; Fluet et al., 2010; Janssen and Scherberger, 2015; Murata et al., 2000, 1997; Raos et al., 2006, 2004; Schaffelhofer et al., 2015). Interestingly, action-related beta power modulation was localized not only within the fronto-parietal pathway traditionally considered to code grasping information, i.e. the dorsolateral pathway, comprising the inferior part of PPC and PMv. This power modulation extended also within the dorsomedial pathway (superior and medial part of PPC and PMd), traditionally considered as coding only reaching information. This finding is supporting convergent monkey (Baumann et al., 2009; Fattori et al., 2012, 2010, 2009; Fluet et al., 2010; Murata et al., 2000, 1997; Raos et al., 2006, 2004) and human studies (Fabbri et al., 2014; Gallivan et al., 2013b, 2011b; Monaco et al., 2014; Verhagen et al., 2008) showing the coding of grasping information within both pathways.

4.2 Effector-independent action coding within fronto-parietal network

Our multivariate analyses showed that local patterns of beta power modulations convey also effector-independent information regarding upcoming actions. At sensor level, this effect was subtended by a specific frequency interval within the more broadband beta power modulation described using univariate analysis. At source level, this effect was localized both within the fronto-parietal network and the ventral stream. Given the different roles attributed to these two cortical pathways, we discuss the possible function of these representations.

With respect to the fronto-parietal network, it is plausible that these action representations might play a direct role in motor control. Previous investigations described similar abstract action representations, i.e. generalizing across different movement features, within human PPC and frontal cortex adopting fMRI (Barany et al., 2014; Gallivan et al., 2013b; Kadmon Harpaz et al., 2014), and

within monkey PMv using single cell recordings (Rizzolatti et al., 1988). Our study extended these results showing that effector-independent information about upcoming action is encoded by beta oscillations within the PPC, premotor and prefrontal cortices.

It is difficult to clearly define which aspects of a planned action might be represented irrespective of the adopted effector, given the difference between the reaching and the grasping conditions in terms of sensorimotor processing. Effector-independent information might refer to the encoding of the spatial position (Gallivan et al., 2013b, 2011a) and/or the intrinsic properties (shape and size) of the to-be grasped object (Gallivan et al., 2013b). Alternatively, it might be related to representing information about the action itself at a more abstract level, i.e. generalizing across specific features (Gallivan et al., 2013b; Kadmon Harpaz et al., 2014). These abstract action representations have been proposed to represent the aim of the motor output irrespective of the means (i.e. specific muscular pattern) by which it is obtained (Gallivan et al., 2013b; Heed et al., 2011; Leoné et al., 2014; Rizzolatti et al., 1988). The encoding of effector-independent information could be crucial in motor control as it allows the flexible remapping of the aim of an intended behavior through a different motor output, comprising a different muscular pattern or even adopting another effector (e.g. the other hand, the mouth or the foot).

4.3 Effector-independent action coding within temporal regions

Abstract action encoding within temporal cortex, particularly within the lateral occipitotemporal cortex (LOTC), supports the recent proposal of its possible role in motor control (Ariani et al., 2015; Gallivan and Culham, 2015; Gallivan et al., 2014, 2013a; Verhagen et al., 2012, 2008). A recruitment of ventral stream regions during the execution of non-visually guided grasping actions have been demonstrated in monkey (Kilintari et al., 2014) and human neuroimaging studies (Astafiev et al., 2004; Orlov et al., 2010; Singhal et al., 2013). This recruitment has been interpreted

as a rehearsal of a high order visual representation of the performed action and/or of the object to be grasped. Furthermore, MVPA analysis of fMRI data within the ventral stream showed encoding of action representations even during movement planning and even if the activity of these regions was below or at baseline level (Ariani et al., 2015; Gallivan et al., 2013a). This suggests that these regions did encode action information even before movement execution. A direct evidence of the causal involvement of temporal regions in performing delayed non-visually guided movements comes also from a recent TMS study (Cohen et al., 2009). TMS perturbation of lateral occipital complex had an effect on kinematics of non-visually guided actions, only when grasping had to be performed after a delay of two seconds, but not if the movement was performed immediately. This specific perturbation effect suggests that information coming from the ventral stream might be particularly crucial in the case of a non-visually guided delayed movement (as the one adopted in our study). Our data support a similar recruitment within the temporal cortex during movement planning. In our specific case, participants had to plan and perform non-visually guided actions without direct visual information regarding the to-be-grasped object. The recruitment of temporal regions might provide the dorsal stream with a "surrogate" source of input, i.e. an abstract representation of the to-be-executed action and/or of the object's properties (i.e. shape and position), for performing the upcoming action (see also Lingnau and Downing, 2015). Our results and other recent investigations (Bracci and Peelen, 2013; Bracci et al., 2011; Gallivan et al., 2014, 2013a; Gutteling et al., 2015; Valyear and Culham, 2010; Verhagen et al., 2012, 2008) support a relevant role of the ventral stream in motor control, which might be involved in coding action or specific learned properties of the target object, especially when this environmental information is not available during action planning. This information might be transferred between ventral and dorsal stream in order to form a motor program (Verhagen et al., 2008).

In line with our current results, Tucciarelli et al. (2015) found abstract (i.e. effector independent) action representations for observed actions in the LOTC. In contrast to the current study, this representation was subtended by modulations within the theta/low alpha band, suggesting possible

differences within the LOTC for observing and acting. Similarly, Tan et al. (2013) showed that occipito-temporal alpha modulations underlay a continuous process for extracting information from observed movements in order to plan a subsequent motor response. These occipitotemporal alpha modulations were also strongly predictive of the subsequent response before its execution, suggesting that incoming information was processed initially within occipitotemporal cortex and, at a later stage, integrated with the planned movement within fronto-parietal areas.

Based on these findings, as alpha band involvement was clearly present also in our univariate and multivariate results, an intriguing hypothesis could be that it underlay the interplay between the neural dynamics of movement planning and observation within the temporal lobe, but further studies are needed to verify this possibility.

4.4 Conclusions

Our univariate approach provided new insights on the coding and the possible integration of different neural representation during movement planning within the fronto-parietal network. Furthermore, our multivariate analysis suggested that the beta band might support "abstract" action encoding localized within the fronto-parietal network and the occipito-temporal cortex. Caution is needed when interpreting decoding data, as MVP analysis is susceptible of discriminating between conditions based on any (experimentally manipulated or not) difference between them. For this reason, our experimental paradigm was devised to control for visual stimulation during the planning phase minimizing potential confounds in interpretation. Keeping in mind the limitations of this approach, our study showed also the potential of MVP analysis as a powerful tool for disentangling different processes simultaneously acting during movement planning by decoding modulations in local patterns of activity.

To conclude, our data support and widen previous investigations on motor control by demonstrating the crucial role of beta oscillations in processing different movement features, spanning from the representation of the adopted effector up to an effector-independent representation of the upcoming action.

Acknowedgements

References

Ariani, G., Wurm, M.F., Lingnau, A., 2015. Decoding Internally and Externally Driven Movement Plans. J. Neurosci. 35, 14160–14171. doi:10.1523/JNEUROSCI.0596-15.2015

Astafiev, S. V, Stanley, C.M., Shulman, G.L., Corbetta, M., 2004. Extrastriate body area in human occipital cortex responds to the performance of motor actions. Nat. Neurosci. 7, 542–548. doi:10.1038/nn1241

Barany, D., Della-Maggiore, V., Viswanathan, S., Cieslak, M., Grafton, S.T., 2014. Feature interactions enable decoding of sensorimotor transformations for goal-directed movement. J. Neurosci. 34, 6860–73. doi:10.1523/JNEUROSCI.5173-13.2014

Baumann, M.A., Fluet, M.C., Scherberger, H., 2009. Context-specific grasp movement representation in the macaque anterior intraparietal area. J. Neurosci. 29, 6436–6448. doi:10.1523/JNEUROSCI.5479-08.2009

Bonini, L., Rozzi, S., Serventi, F.U., Simone, L., Ferrari, P.F., Fogassi, L., 2010. Ventral premotor and inferior parietal cortices make distinct contribution to action organization and intention understanding. Cereb. Cortex 20, 1372–85. doi:10.1093/cercor/bhp200

Bonini, L., Serventi, F.U., Simone, L., Rozzi, S., Ferrari, P.F., Fogassi, L., 2011. Grasping neurons of monkey parietal and premotor cortices encode action goals at distinct levels of abstraction during complex action sequences. J. Neurosci. 31, 5876–86. doi:10.1523/JNEUROSCI.5186-10.2011

Bonini, L., Ugolotti Serventi, F., Bruni, S., Maranesi, M., Bimbi, M., Simone, L., Rozzi, S., Ferrari, P.F., Fogassi, L., 2012. Selectivity for grip type and action goal in macaque inferior parietal and ventral premotor grasping neurons. J. Neurophysiol. 108, 1607–19. doi:10.1152/jn.01158.2011

Bracci, S., Cavina-Pratesi, C., Ietswaart, M., Caramazza, A., Peelen, M. V, 2011. Closely overlapping responses to tools and hands in the left lateral occipitotemporal cortex. J. Vis. doi:10.1167/11.11.813

Bracci, S., Peelen, M. V., 2013. Body and Object Effectors: The Organization of Object Representations in High-Level Visual Cortex Reflects Body-Object Interactions. J. Neurosci. 33, 18247–18258. doi:10.1523/JNEUROSCI.1322-13.2013

Brainard, D.H., 1997. The Psychophysics Toolbox. Spat. Vis. 10, 433–436. doi:10.1163/156856897X00357

Brinkman, L., Stolk, A., Dijkerman, H.C., de Lange, F.P., Toni, I., 2014. Distinct roles for alpha- and beta-band oscillations during mental simulation of goal-directed actions. J Neurosci 34, 14783–14792. doi:10.1523/JNEUROSCI.2039-14.2014

Brochier, T., Umiltà, M.A., 2007. Cortical control of grasp in non-human primates. Curr. Opin. Neurobiol. 17, 637–43. doi:10.1016/j.conb.2007.12.002

Chang, C., Lin, C., 2011. LIBSVM : A Library for Support Vector Machines. ACM Trans. Intell. Syst. Technol. 2, 1–39. doi:10.1145/1961189.1961199

Cheyne, D.O., 2013. MEG studies of sensorimotor rhythms: A review. Exp. Neurol. 245, 27–39. doi:10.1016/j.expneurol.2012.08.030

Cohen, N.R., Cross, E.S., Tunik, E., Grafton, S.T., Culham, J.C., 2009. Ventral and dorsal stream contributions to the online control of immediate and delayed grasping: a TMS approach.

Neuropsychologia 47, 1553–62. doi:10.1016/j.neuropsychologia.2008.12.034

Culham, J.C., Cavina-Pratesi, C., Singhal, A., 2006. The role of parietal cortex in visuomotor control: what have we learned from neuroimaging? Neuropsychologia 44, 2668–84. doi:10.1016/j.neuropsychologia.2005.11.003

Culham, J.C., Valyear, K.F., 2006. Human parietal cortex in action. Curr. Opin. Neurobiol. 16, 205–12. doi:10.1016/j.conb.2006.03.005

Fabbri, S., Strnad, L., Caramazza, A., Lingnau, A., 2014. Overlapping representations for grip type and reach direction. Neuroimage 94, 138–46. doi:10.1016/j.neuroimage.2014.03.017

Fattori, P., Breveglieri, R., Marzocchi, N., Filippini, D., Bosco, A., Galletti, C., 2009. Hand orientation during reach-to-grasp movements modulates neuronal activity in the medial posterior parietal area V6A. J. Neurosci. 29, 1928–36. doi:10.1523/JNEUROSCI.4998-08.2009

Fattori, P., Breveglieri, R., Raos, V., Bosco, A., Galletti, C., 2012. Vision for action in the macaque medial posterior parietal cortex. J. Neurosci. 32, 3221–34. doi:10.1523/JNEUROSCI.5358-11.2012

Fattori, P., Raos, V., Breveglieri, R., Bosco, A., Marzocchi, N., Galletti, C., 2010. The dorsomedial pathway is not just for reaching: grasping neurons in the medial parieto-occipital cortex of the macaque monkey. J. Neurosci. 30, 342–9. doi:10.1523/JNEUROSCI.3800-09.2010

Filimon, F., 2010. Human cortical control of hand movements: parietofrontal networks for reaching, grasping, and pointing. Neuroscientist 16, 388–407. doi:10.1177/1073858410375468

Fluet, M.C., Baumann, M.A., Scherberger, H., 2010. Context-specific grasp movement representation in macaque ventral premotor cortex. J. Neurosci. 30, 15175–84. doi:10.1523/JNEUROSCI.3343-10.2010

Gallivan, J.P., Cant, J.S., Goodale, M.A., Flanagan, J.R., 2014. Representation of object weight in human ventral visual cortex. Curr. Biol. 24, 1866–73. doi:10.1016/j.cub.2014.06.046

Gallivan, J.P., Chapman, C.S., McLean, D.A., Flanagan, J.R., Culham, J.C., 2013a. Activity patterns in the category-selective occipitotemporal cortex predict upcoming motor actions. Eur. J. Neurosci. 38, 2408–24. doi:10.1111/ejn.12215

Gallivan, J.P., Culham, J.C., 2015. Neural coding within human brain areas involved in actions. Curr. Opin. Neurobiol. 33, 141–149. doi:10.1016/j.conb.2015.03.012

Gallivan, J.P., McLean, D.A., Flanagan, J.R., Culham, J.C., 2013b. Where one hand meets the other: limb-specific and action-dependent movement plans decoded from preparatory signals in single human frontoparietal brain areas. J. Neurosci. 33, 1991–2008. doi:10.1523/JNEUROSCI.0541-12.2013

Gallivan, J.P., McLean, D.A., Smith, F.W., Culham, J.C., 2011a. Decoding effector-dependent and effector-independent movement intentions from human parieto-frontal brain activity. J. Neurosci. 31, 17149–68. doi:10.1523/JNEUROSCI.1058-11.2011

Gallivan, J.P., McLean, D.A., Valyear, K.F., Culham, J.C., 2013c. Decoding the neural mechanisms of human tool use. Elife 2, e00425. doi:10.7554/eLife.00425

Gallivan, J.P., McLean, D.A., Valyear, K.F., Pettypiece, C.E., Culham, J.C., 2011b. Decoding action intentions from preparatory brain activity in human parieto-frontal networks. J. Neurosci. 31, 9599–610. doi:10.1523/JNEUROSCI.0080-11.2011

Grafton, S.T., 2010. The cognitive neuroscience of prehension: recent developments. Exp. brain

Res. 204, 475–91. doi:10.1007/s00221-010-2315-2

Gross, J., Kujala, J., Hamalainen, M., Timmermann, L., Schnitzler, A., Salmelin, R., 2001. Dynamic imaging of coherent sources: Studying neural interactions in the human brain. Proc. Natl. Acad. Sci. U. S. A. 98, 694–9. doi:10.1073/pnas.98.2.694

Gutteling, T.P., Petridou, N., Dumoulin, S.O., Harvey, B.M., Aarnoutse, E.J., Kenemans, J.L., Neggers, S.F.W., 2015. Action Preparation Shapes Processing in Early Visual Cortex. J. Neurosci. 35, 6472–6480. doi:10.1523/JNEUROSCI.1358-14.2015

Heed, T., Beurze, S.M., Toni, I., Röder, B., Medendorp, W.P., 2011. Functional rather than effector-specific organization of human posterior parietal cortex. J. Neurosci. 31, 3066–76. doi:10.1523/JNEUROSCI.4370-10.2011

Janssen, P., Scherberger, H., 2015. Visual Guidance in Control of Grasping. Annu. Rev. Neurosci. 38, 150403170110009. doi:10.1146/annurev-neuro-071714-034028

Kadmon Harpaz, N., Flash, T., Dinstein, I., 2014. Scale-invariant movement encoding in the human motor system. Neuron 81, 452–461. doi:10.1016/j.neuron.2013.10.058

Kilavik, B.E., Zaepffel, M., Brovelli, A., MacKay, W. a, Riehle, A., 2013. The ups and downs of β oscillations in sensorimotor cortex. Exp. Neurol. 245, 15–26. doi:10.1016/j.expneurol.2012.09.014

Kilintari, M., Raos, V., Savaki, H.E., 2014. Involvement of the superior temporal cortex in action execution and action observation. J. Neurosci. 34, 8999–9011. doi:10.1523/JNEUROSCI.0736-14.2014

Koch, G., Cercignani, M., Pecchioli, C., Versace, V., Oliveri, M., Caltagirone, C., Rothwell, J., Bozzali, M., 2010. In vivo definition of parieto-motor connections involved in planning of grasping movements. Neuroimage 51, 300–12. doi:10.1016/j.neuroimage.2010.02.022

Kriegeskorte, N., Bandettini, P., 2007. Combining the tools: activation- and information-based fMRI analysis. Neuroimage 38, 666–8. doi:10.1016/j.neuroimage.2007.06.030

Kriegeskorte, N., Simmons, W.K., Bellgowan, P.S.F., Baker, C.I., 2009. Circular analysis in systems neuroscience: the dangers of double dipping. Nat. Neurosci. 12, 535–540. doi:10.1167/8.6.88

Leo, A., Handjaras, G., Bianchi, M., Marino, H., Gabiccini, M., Guidi, A., Scilingo, E.P., Pietrini, P., Bicchi, A., Santello, M., Ricciardi, E., 2016. A synergy-based hand control is encoded in human motor cortical areas. Elife 5, 1–32. doi:10.7554/eLife.13420

Leoné, F.T.M., Heed, T., Toni, I., Medendorp, W.P., 2014. Understanding effector selectivity in human posterior parietal cortex by combining information patterns and activation measures. J. Neurosci. 34, 7102–12. doi:10.1523/JNEUROSCI.5242-13.2014

Lingnau, A., Downing, P.E., 2015. The lateral occipitotemporal cortex in action. Trends Cogn. Sci. 19, 268–277. doi:10.1016/j.tics.2015.03.006

Maris, E., Oostenveld, R., 2007. Nonparametric statistical testing of EEG- and MEG-data. J. Neurosci. Methods 164, 177–90. doi:10.1016/j.jneumeth.2007.03.024

Monaco, S., Sedda, A., Cavina-Pratesi, C., Culham, J.C., 2014. Neural correlates of object size and object location during grasping actions. Eur. J. Neurosci. 1–12. doi:10.1111/ejn.12786

Murata, A., Fadiga, L., Fogassi, L., Gallese, V., Raos, V., Rizzolatti, G., 1997. Object representation in the ventral premotor cortex (area F5) of the monkey. J. Neurophysiol. 78, 2226–30.

Murata, A., Gallese, V., Luppino, G., Kaseda, M., Sakata, H., 2000. Selectivity for the shape, size, and orientation of objects for grasping in neurons of monkey parietal area AIP. J. Neurophysiol. 83, 2580–601.

Nolte, G., 2003. The magnetic lead field theorem in the quasi-static approximation and its use for magnetoencephalography forward calculation in realistic volume conductors. Phys. Med. Biol. 48, 3673–3652.

Oostenveld, R., Fries, P., Maris, E., Schoffelen, J.-M., 2011. FieldTrip: Open source software for advanced analysis of MEG, EEG, and invasive electrophysiological data. Comput. Intell. Neurosci. 2011, 156869. doi:10.1155/2011/156869

Oosterhof, N.N., Connolly, A.C., Haxby, J. V, 2016. CoSMoMVPA : multi-modal multivariate pattern analysis of neuroimaging data in Matlab / GNU Octave.

Oosterhof, N.N., Tipper, S.P., Downing, P.E., 2012a. Viewpoint (in)dependence of action representations: an MVPA study. J. Cogn. Neurosci. 24, 975–89. doi:10.1162/jocn_a_00195

Oosterhof, N.N., Tipper, S.P., Downing, P.E., 2012b. Visuo-motor imagery of specific manual actions: a multi-variate pattern analysis fMRI study. Neuroimage 63, 262–71. doi:10.1016/j.neuroimage.2012.06.045

Oosterhof, N.N., Wiestler, T., Downing, P.E., Diedrichsen, J., 2011. A comparison of volume-based and surface-based multi-voxel pattern analysis. Neuroimage 56, 593–600. doi:10.1016/j.neuroimage.2010.04.270

Oosterhof, N.N., Wiggett, A.J., Diedrichsen, J., Tipper, S.P., Downing, P.E., 2010. Surface-based information mapping reveals crossmodal vision-action representations in human parietal and occipitotemporal cortex. J. Neurophysiol. 104, 1077–89. doi:10.1152/jn.00326.2010

Orlov, T., Makin, T.R., Zohary, E., 2010. Topographic representation of the human body in the occipitotemporal cortex. Neuron 68, 586–600. doi:10.1016/j.neuron.2010.09.032

Pelli, D.G., 1997. The VideoToolbox software for visual psychophysics: transforming numbers into movies. Spat. Vis. 10, 437–442.

Pernet, C.R., Latinus, M., Nichols, T.E., Rousselet, G.A., 2015. Cluster-based computational methods for mass univariate analyses of event-related brain potentials/fields: A simulation study. J. Neurosci. Methods 250, 85–93. doi:10.1016/j.jneumeth.2014.08.003

Raos, V., Umiltá, M.-A., Gallese, V., Fogassi, L., 2004. Functional properties of grasping-related neurons in the dorsal premotor area F2 of the macaque monkey. J. Neurophysiol. 92, 1990–2002. doi:10.1152/jn.00154.2004

Raos, V., Umiltá, M.-A., Murata, A., Fogassi, L., Gallese, V., 2006. Functional properties of grasping-related neurons in the ventral premotor area F5 of the macaque monkey. J. Neurophysiol. 95, 709–29. doi:10.1152/jn.00463.2005

Rizzolatti, G., Camarda, R., Fogassi, L., Gentilucci, M., Luppino, G., Matelli, M., 1988. Functional organization of inferior area 6 in the macaque monkey. Exp. brain Res. 71, 491–507.

Schaffelhofer, S., Agudelo-toro, A., Scherberger, H., 2015. Decoding a Wide Range of Hand Configurations from Macaque Motor, Premotor, and Parietal Cortices. J. Neurosci. 35, 1068–1081. doi:10.1523/JNEUROSCI.3594-14.2015

Schwarzbach, J., 2011. A simple framework (ASF) for behavioral and neuroimaging experiments based on the psychophysics toolbox for MATLAB. Behav. Res. Methods 43, 1194–201. doi:10.3758/s13428-011-0106-8

Singhal, A., Monaco, S., Kaufman, L.D., Culham, J.C., 2013. Human fMRI reveals that delayed action re-recruits visual perception. PLoS One 8, e73629. doi:10.1371/journal.pone.0073629

Smith, S.M., Nichols, T.E., 2009. Threshold-free cluster enhancement: Addressing problems of smoothing, threshold dependence and localisation in cluster inference. Neuroimage 44, 83–98. doi:10.1016/j.neuroimage.2008.03.061

Spinks, R.L., Kraskov, A., Brochier, T., Umilta, M.A., Lemon, R.N., 2008. Selectivity for grasp in local field potential and single neuron activity recorded simultaneously from M1 and F5 in the awake macaque monkey. J. Neurosci. 28, 10961–71. doi:10.1523/JNEUROSCI.1956-08.2008

Tan, H.R.M., Leuthold, H., Gross, J., 2013. Gearing up for action: Attentive tracking dynamically tunes sensory and motor oscillations in the alpha and beta band. Neuroimage 82, 634–644. doi:10.1016/j.neuroimage.2013.04.120

Tucciarelli, R., Turella, L., Oosterhof, N.N., Weisz, N., Lingnau, A., 2015. MEG Multivariate Analysis Reveals Early Abstract Action Representations in the Lateral Occipitotemporal Cortex. J. Neurosci. 35, 16034–16045. doi:10.1523/JNEUROSCI.1422-15.2015

Turella, L., Lingnau, A., 2014. Neural correlates of grasping. Front. Hum. Neurosci. 8, 686. doi:10.3389/fnhum.2014.00686

Tzagarakis, C., Ince, N.F., Leuthold, A.C., Pellizzer, G., 2010. Beta-band activity during motor planning reflects response uncertainty. J. Neurosci. 30, 11270–7. doi:10.1523/JNEUROSCI.6026-09.2010

Valyear, K.F., Culham, J.C., 2010. Observing Learned Object-specific Functional Grasps Preferentially Activates the Ventral Stream. J. Cogn. Neurosci. 22, 970–984. doi:10.1162/jocn.2009.21256

Van Der Werf, J., Jensen, O., Fries, P., Medendorp, W.P., 2010. Neuronal synchronization in human posterior parietal cortex during reach planning. J. Neurosci. 30, 1402–12. doi:10.1523/JNEUROSCI.3448-09.2010

Van Essen, D.C., Drury, H.A., Dickson, J., Harwell, J., Hanlon, D., Anderson, C.H., 2001. An Integrated Software Suite for Surface-based Analyses of Cerebral Cortex. J. Am. Med. Informatics Assoc. 8, 443–459. doi:10.1136/jamia.2001.0080443

Vargas-Irwin, C.E., Franquemont, L., Black, M.J., Donoghue, J.P., 2015. Linking Objects to Actions: Encoding of Target Object and Grasping Strategy in Primate Ventral Premotor Cortex. J. Neurosci. 35, 10888–10897. doi:10.1523/JNEUROSCI.1574-15.2015

Verhagen, L., Dijkerman, H.C., Grol, M.J., Toni, I., 2008. Perceptuo-motor interactions during prehension movements. J. Neurosci. 28, 4726–35. doi:10.1523/JNEUROSCI.0057-08.2008

Verhagen, L., Dijkerman, H.C., Medendorp, W.P., Toni, I., 2012. Cortical dynamics of sensorimotor integration during grasp planning. J. Neurosci. 32, 4508–19. doi:10.1523/JNEUROSCI.5451-11.2012

Vesia, M., Bolton, D. a, Mochizuki, G., Staines, W.R., 2013. Human parietal and primary motor cortical interactions are selectively modulated during the transport and grip formation of goal-directed hand actions. Neuropsychologia 51, 410–7. doi:10.1016/j.neuropsychologia.2012.11.022

Vesia, M., Crawford, J.D., 2012. Specialization of reach function in human posterior parietal cortex. Exp. brain Res. 221, 1–18. doi:10.1007/s00221-012-3158-9

Virji-Babul, N., Moiseev, A., Cheung, T., Weeks, D., Cheyne, D., Ribary, U., 2010. Spatial-temporal dynamics of cortical activity underlying reaching and grasping. Hum. Brain Mapp.

31, 160–71. doi:10.1002/hbm.20853

Wheaton, L., Fridman, E., Bohlhalter, S., Vorbach, S., Hallett, M., 2009. Left parietal activation related to planning, executing and suppressing praxis hand movements. Clin. Neurophysiol. 120, 980–6. doi:10.1016/j.clinph.2009.02.161

Wheaton, L., Shibasaki, H., Hallett, M., 2005. Temporal activation pattern of parietal and premotor areas related to praxis movements. Clin. Neurophysiol. 116, 1201–12. doi:10.1016/j.clinph.2005.01.001

Wurm, M.F., Ariani, G., Greenlee, M.W., Lingnau, A., 2015. Decoding Concrete and Abstract Action Representations During Explicit and Implicit Conceptual Processing. Cereb. Cortex bhv169. doi:10.1093/cercor/bhv169

Wurm, M.F., Lingnau, A., 2015. Decoding actions at different levels of abstraction. J. Neurosci. 35, 7727–35. doi:10.1523/JNEUROSCI.0188-15.2015

Zaepffel, M., Trachel, R., Kilavik, B.E., Brochier, T., 2013. Modulations of EEG beta power during planning and execution of grasping movements. PLoS One 8, e60060. doi:10.1371/journal.pone.0060060

Highlights

- MEG was adopted to investigate the neural dynamics of movement planning.
- Action and effector information is reflected by beta band power modulations.
- Action and effector-related modulations were found in fronto-parietal regions.
- Multivariate analysis showed encoding of effector-independent action information.
- This encoding was localized within fronto-parietal and temporal regions.